INTERNATIONAL JOURNAL OF OPTIMIZATION IN CIVIL ENGINEERING
Int. J. Optim. Civil Eng., 2014; 4(3):293-308

OPTIMAL GROUND MOTION SCALING USING ENHANCED SWARM INTELLIGENCE FOR SIZING DESIGN OF STEEL FRAMES

M. Shahrouzi[1*,†] and A. Mohammadi[2]
[1]*Faculty of Engineering, Kharazmi University, Tehran, Iran*
[2]*Road, Housing and Urban Development Research Centre, Tehran, Iran*

ABSTRACT

Dynamic structural responses via time history analysis are highly dependent to characteristics of selected records as the seismic excitation. Ground motion scaling is a well-known solution to reduce such a dependency and increase reliability to the dynamic results. The present work, formulate a twofold problem for optimal spectral matching and performing consequent sizing optimization based on such scaled ground motion via numerical step-by-step analyses. Particle swarm optimization as a widely used meta-heuristic is specialized and improved to solve this problem treating a number of examples. The scaling error is evaluated using both traditional procedure and the developed method. In this regard, some issues are studied including the effect of structural period and shape of the design spectrum on the results. Contribution of the proposed enhancement on the standard particle swarm intelligence has improved its explorative capability resulting in higher efficiency of the algorithm.

Received: 3 March 2014; Accepted: 10 September 2014

KEY WORDS: spectral matching; particle swarm optimization; time history analysis; sizing optimization; shear building.

1. INTRODUCTION

Several code-specific or practical procedures in the seismic design or vulnerability assessment require earthquake time-history records for the step-by-step analysis procedures

*Corresponding author: Faculty of Engineering, Kharazmi University, Tehran, Iran
†E-mail address: shahruzi@khu.ac.ir (M. Shahrouzi)

[1-3]. It includes analysis of non-linear systems for which superposition is not reasonable [3-4]. The main challenge to use time-history input records is case-dependency of them and impossibility of earthquake prediction. Hence, a unique source of decision making based on time history analysis is not available because the structural responses varies as the input record is changed. On the other hand, well-known seismic codes have introduced a number of linear spectra as a legal input source of design.

One solution for this problem is to make pure artificial records and filter them according to the site characteristics [4, 5] or to reconstruct the real record so that its spectrum fit the target standard [6, 7]. None of these approaches preserve frequency content and many other seismic characteristics of the recorded earthquake signal. According to the common practice in the seismic codes, a set of real records are scaled by their amplitudes in order to match a target standard spectrum [8-10]. As the smooth design spectrum is constructed on a statistical basis covering a variety of previous earthquakes, no single one may exactly match it. Common manual/code-practice accepts equal scaling coefficients for all the records in such a set which usually causes considerable compatibility error in the resulting scaled spectrum with respect to the target.

Reduction of such an error is concerned here by optimizing the scaling factor for any selected set of earthquake accelerograms distinctly. These real-valued factors are measured with respect to each other, thus the cardinality of such a continuous design space is infinity. The matter emphasizes necessity of using efficient algorithms to deal with such a continuous problem.

In this regard, the present work offers an improved search algorithm in the category of swarm intelligence which mimics the behaviour of natural swarms such as bird flocks or ant colonies to achieve their desired goal [11-19]. The efficiency and effectiveness of the developed method is then evaluated in a number of examples showing its superiority over the common practice according to the seismic design code. Further sizing design is performed using the obtained sets of scale factors to evaluate economical contribution of optimal ground motion scaling on structural design of building frames.

2. PROBLEM FORMULATION

2.1 Spectral matching optimization

Suppose a set of N horizontal earthquakes is given. At this stage, N single spectra are provided whose weighted average should not fall below the target spectrum according to the Iranian code of seismic design ICPSRDB 2800-05 [1]. The optimization problem of spectral matching is thus formulated as follows to tune the weighting factors, α_i:

$$\begin{aligned} &Maximize \quad F(\alpha_1,...,\alpha_N) = 1/Err \\ &S.t. \qquad\quad 0.5 \le \alpha_i \le 2.0 \end{aligned} \tag{1}$$

for which F denotes the fitness function and the matching error, Err, is computed as:

$$Err = 100\sqrt{\frac{1}{N}\sum_{T=T_1}^{T_2}\left(\frac{Sa_{Target}(T) - \beta.Spa_{avg}(T)}{Sa_{Target}(T)}\right)^2} \tag{2a}$$

$$Spa_{avg}(T) = \frac{1}{N}\sum_{i=1}^{N}\alpha_i SA_i(T) \tag{2b}$$

and β imposes the mean spectrum, $Spa_{avg}(T)$, to fall equal or greater than the target within the specified period interval. It is calculated as:

$$\beta = \max_T\left\{\frac{Sa_{Target}(T)}{Spa_{avg}(T)}\right\} \tag{3}$$

2.2 Frame sizing optimization

Once a set of scale factors for the employed earthquake records is determined either manually (equal factors) or via the spectral matching optimization, another issue is activated; that is to optimize the building frame sections under the scaled ground motion.

In this regard, the dynamic results should be further combined with the static response of the structure under gravitational loading (e.g. dead and live loads). If *N* is less than 7 the maximum response out of *N* dynamic excitations is used; otherwise the mean dynamic response is considered according to the seismic design code ICPSRDB 2800-05.

The new optimization problem is to minimize the structural weight for the assigned frame sections providing that all the addressing stress/displacement limitations of the design code are satisfied. In this study the allowable stress design requirements due to AISC-ASD89 and ICPSRDB 2800-05 are employed. The following penalty function is used to evaluate equivalent fitness function.

$$Fitness = -f(x_1,...,x_m)*(1+K_p\sum C_l) \tag{4}$$

in which *f* stands for the objective function (weight), C_l denotes the l^{th} constraint violation and K_p is the employed penalty coefficient. The section indices assigned to the *m* member groups are denoted by $\underline{X} =< x_1,...,x_m >$ as the structural design vector.

Here-in-after any frame is modeled as a shear building with one horizontal degree of freedom at each storey level which is considered a rigid floor. In order to indirectly apply the geometric constraint, section indices in the design vector are sorted in descending order before fitness evaluation; that is to insure no column section in any lower storey is lighter than the upper storey column.

3. SWARM INTELLIGENCE BASICS

Complexity of many engineering problems has made the investigators to approach meta-heuristic search; the algorithms usually inspired by artificial behaviour of natural

populations to seek their proper goals. Swarm intelligence is based on two main capabilities of the searching agents: self organization and stigmergy. The former enables any particle in the swarm to move; i.e. to alter a solution candidate during optimization based on its own experience. Stigmergy stands for the effect of environment on an agent which is addressed by gathering information from the solution candidates discovered by other search agents.

One of the well-known algorithms in the swarm intelligence category is Particle Swarm Optimization, PSO, introduced by Eberhart and Kennedy [11, 12]. Any search agent in PSO is called a particle taking its location vector X a point or solution candidate in the search space. After completing the random initiation of the particles' population with a predetermined size, any new solution at the next iteration *k+1*, is discovered by the particle *i* using the following relations:

$$\underline{X}_i^{k+1} = \underline{X}_i^{k} + \underline{V}_i^{k} \tag{5}$$

$$\underline{V}_i^{k+1} = c_i \underline{V}_i^{k} + r.c_c(\underline{X}_i^{Pbest} - \underline{X}_i^{k}) + r.c_s(\underline{X}^{Gbets} - \underline{X}_i^{k}) \tag{6}$$

in which c_i, c_c, c_s stand for inertial, cognitive and social factors and r is a function giving random numbers between 0 and 1. $\underline{X}_i^{Pbest}$ denotes the best pervious position that a particle has already experienced while $\underline{X}^{gbest}$ is the global best position among the entire swarm. The former mimics the cognitive and the latter models social relations in a natural (bird's) swarm to find the optimal position.

Such a terminology can be used in the following optimization algorithm:

1. Select PSO parameters: $PopSize$, $NumIters$, c_i, c_c, c_s
2. Initiate $PopSize$ number of solution candidates and their velocity vectors, $\underline{V}_i$, randomly.
3. Evaluate the particles fitness values
4. Determine the best position experienced by each i^{th} particle during its search as $\underline{X}_i^{Pbest}$
5. Identify $\underline{X}^{gbest}$ as the fittest $\underline{X}_j^{Pbest}$ among all current swarm particles using:

$$j = \arg(\max_i(Fitness(\underline{X}_i^{Pbest}))) \tag{7}$$

6. Reposition particles according to Eq.6 to form new population of particles
7. Repeat the steps 3 to 6 for a predetermined $NumIters$ number of iterations.

4. ENHANCED PARTICLE SWARM OPTIMIZER

Performance of a meta-heuristic algorithm highly depends on proper balance between intensification and diversification. Intensification provides exploitation or local search capability while diversification is also needed to explore new parts of the search space.

In this regard, a modified version of the algorithm, called MPSO, is offered here substituting the Eq.6 with the following relation:

$$\underline{V}_i^{k+1} = r.c_i \underline{V}_i^k + r.c_c(\underline{X}_i^{Pbest} - \underline{X}_i^k) + r.c_s(\underline{X}^{Gbets} - \underline{X}_i^k) + (1 - \frac{k}{NumItr}) r.c_R(\underline{X}_R^k - \underline{X}_i^k) \quad (8)$$

In the above relation three modification strategies are employed to enhance the standard PSO: First, a random generator is added to the inertial term providing more exploration during the search. As the second strategy, passive congregation [16] is employed by an additional movement toward $\underline{X}_R^k$; denoting a randomly picked particle over the current swarm. The last improvement is multiplying the 4th term factor, c_R, by linearly degrading agent $(1 - \frac{k}{NumItr})$.

These modifications are designated to add more diversification in early stages of the search and more intensification as the search progress in order not to loose the near optimal solution found in the last iterations. Fig. 1 shows flowchart of the proposed MPSO while its performance is tested and compared with the standard PSO in the next section.

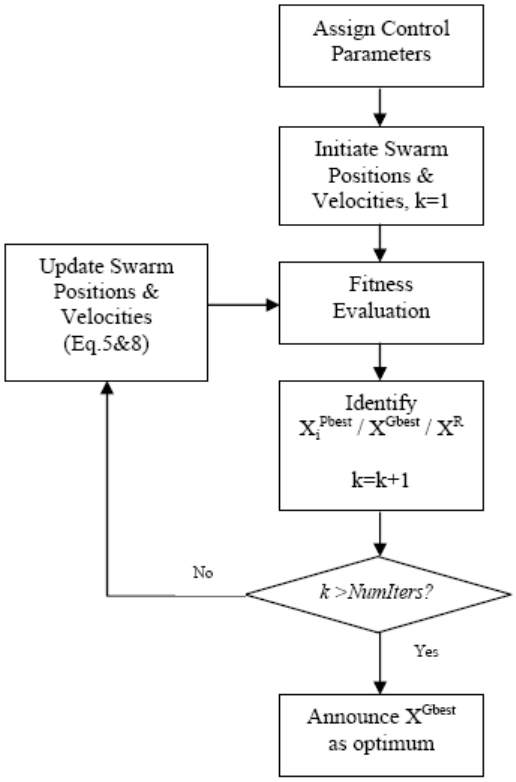

Figure 1. Flowchart of the proposed optimization algorithm

5. NUMERICAL EXAMPLES

A 6-storey and a 13-storey steel frame, both with 2-bays are treated to illustrate the concepts of this study over low- and medium-rise buildings. Typical storey height and bay length are

3 and 5 meters, respectively. The floor masses are computed using the uniform dead load plus 20% of the live load. During optimization, every member group is assigned a structural profile among 31 European standard Sections as listed in Table 1. All the sections are constructed from steel grade St-37. For the sake of more computational efficiency during several dynamic analyses and to reduce the search space size, member grouping is fixed at every storey as depicted in Fig. 2.

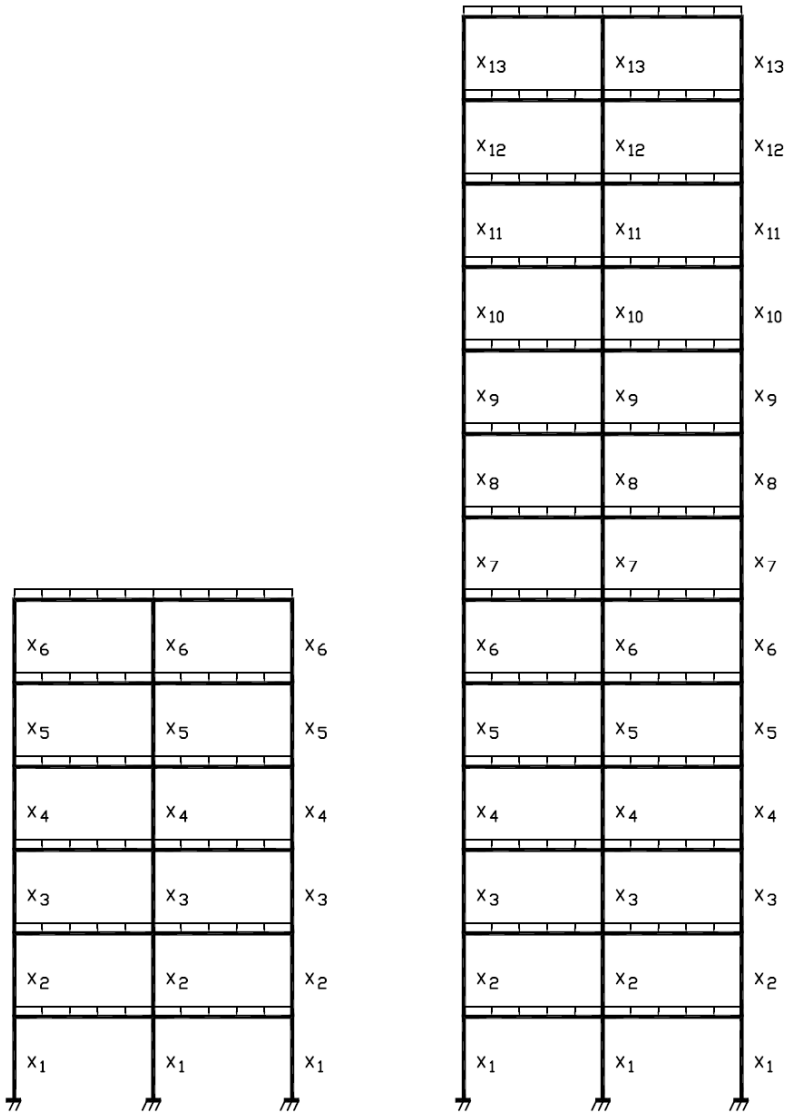

Figure 2. Member grouping for (a) 6 storey-2 bay and (b) 13 storey-2 bay frames with rigid floors

Table 1: Section list for sizing optimization

Section Index	Section Name	Section Index	Section Name	Section Index	Section Name
1	IPE120	12	IPE400	23	TUBO220X220X20
2	IPE140	13	IPE450	24	TUBO240X240X20
3	IPE160	14	IPE500	25	TUBO260X260X20
4	IPE180	15	IPE550	26	TUBO280X280X20
5	IPE200	16	IPE600	27	TUBO300X300X20
6	IPE220	17	TUBO100X100X10	28	TUBO320X320X20
7	IPE240	18	TUBO120X120X20	29	TUBO340X340X20
8	IPE270	19	TUBO140X140X20	30	TUBO380X380X20
9	IPE300	20	TUBO160X160X20	31	TUBO400X400X25
10	IPE330	21	TUBO180X180X20		
11	IPE360	22	TUBO200X200X20		

Stress and drift constraints are evaluated under combined static gravitational and dynamic seismic loading. The allowable storey drift are determined regarding Iranian Standard 2800 whereas the building frame is assumed to have a behavior factor of $R = 5$ and be located at the *very high* seismic zone. Combined bending and axial stress ratios are evaluated using the AISC-ASD89 procedure [20].

Gravitational loading includes dead load of 25 $\frac{kgf}{cm}$ and live load of $5\frac{kgf}{cm}$ uniformly exerted on the floor beams. Meanwhile, the dynamic loading is implemented as the base excitation using a set of 7 accelerograms as given in Table 2 taken from PEER strong ground motion database [21]. Variety of resulted spectra can be observed in Fig. 3. They are generated for 5% damping ratio as offered in the design code [1]. Each accelerogram is scaled before being used in the dynamic analysis using either method: manual practice, optimized with PSO or with MPSO. In the manual/code practice all y_i factors are taken unity then scaled by β to construct equal scale factors so that the resulting mean spectra do not fall below the target within the period range: $0.2T_{Structure} \sim 1.5T_{Structure}$. Such a period interval is due to ICPSRDB 2800-05 dependent to the $T_{Structure}$ estimated based on the frame's total height (in meters), H, using the following design code relation [1]:

$$T_{Structure} = 0.08H^{0.75} \tag{9}$$

Table 2: The set of earthquake components for spectral matching

Record	1	2	3	4	5	6	7
Location	Cape Mendocino	Landers	Northridge	Northridge	Cape Mendocino	Tabas	Tabas
Date	1992-4-25	1992-6-28	1994-1-17	1994-1-17	1992-4-25	1978-9-16	1978-9-16
Station	Petrolia	Yermo	NewHall	Tarzana	Rio	Dayhook	Tabas

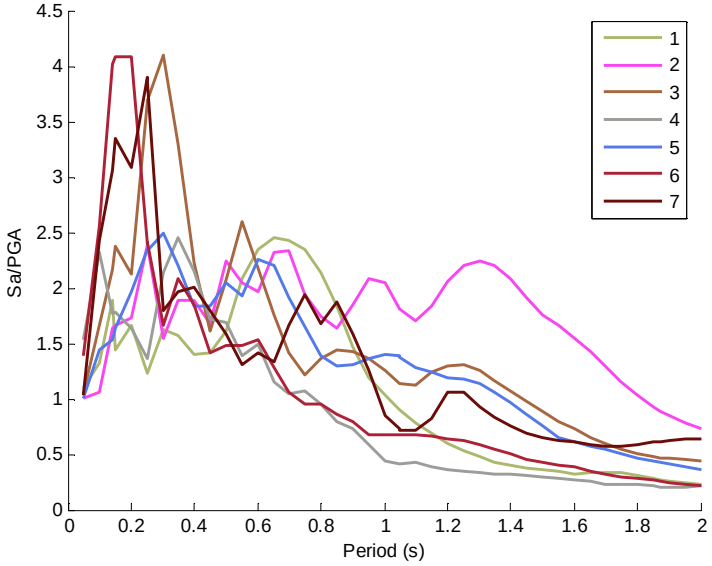

Figure 3. Normalized spectra of the employed earthquakes for 5% damping

In the spectral matching optimization, the y_i factors are derived using a presented swarm intelligent algorithm and then multiplied by proper β to generate the resulting set of scale factors.

Before scaling, each accelerogram is normalized to its peak ground acceleration, PGA. Thus the seismic hazard effect due to the design base earthquake and seismicity of the site zone should be taken into consideration prior to dynamic analysis. In addition, nonlinear effects are indirectly estimated by the structural behavior factor R according to the allowable stress design procedure of ICPSRDB 2800-05. Hence, the normalized accelerograms not only are scaled by the factors resulted from spectral matching but also are further multiplied by $\gamma = PGA.I/R$ to be used in the linear step-by-step analysis. Here, the building importance factor I is taken 1 while $PGA = 0.35g$ for very high seismic zone due to ICPSRDB 2800-05.

Table 3 gives the control parameters used for PSO and MPSO during spectral matching and sizing optimization. Notify that c_R is only used in MPSO. A Diversity Index, DI, is also defined as the coefficient of variation among the population of design vectors. The randomly initiated population is identically employed for both algorithms in every comparison. A penalty coefficient of $K_P = 100$ is used for the sizing design to insure satisfaction of structural constraints.

Table 3: The employed control parameters for optimization

Problem	Algorithm	*PopSize*	*NumIters*	c_i	c_c	c_s	c_R
Spectral Matching	PSO	10	150	1	1	1	-
	MPSO	10	150	1	1	1	4
Frame Sizing	PSO	20	100	1	1	1	-
	MPSO	20	100	1	1	1	4

5.1 The 6-storey 2-bay example

For the first test, the normalized spectrum of ICPSRDB 2800-05 using soil type I is considered as the target for spectral matching within the period interval: $0.060 \sim 0.445\,\mathrm{s}$. The natural period of this structure is $0.699\,\mathrm{s}$ based on Eq. 9. Results of the three scaling methods are compared against the target in Fig. 4 whereas the period interval is identified by the dashed lines. As declared in this figure, the results are considerably closer to the design spectrum for optimized cases than manual; however, all of them satisfy to be over the target spectrum in the suited period interval. It can also be realized that the MPSO method has resulted in the most compatible spectrum with the target among the three methods. Fig. 5 better shows superiority of the MPSO over PSO in achieving higher fitness during spectral matching optimization. Table 4 declares that the three employed scaling methods have resulted in three scale factor sets different from each other. According to Table 5, the manual practice has resulted in about 27% spectral compatibility error while it is reduced to 19% and 15% for PSO and MPSO, respectively. Such a variation in the scaling factors and the resulting errors, confirms importance of optimization in this problem.

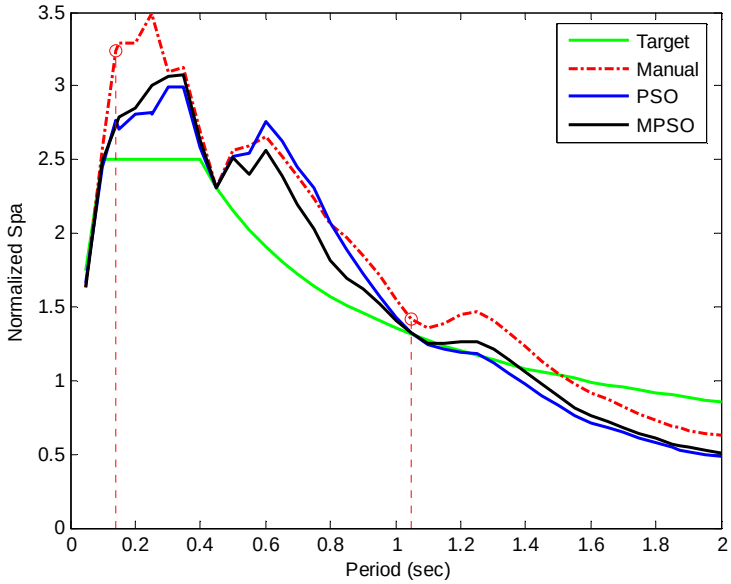

Figure 4. Comparison of various mean scaled spectra matched for the period interval of 6 storey-2 bay frame example with the target design spectrum (5% damped - soil type I)

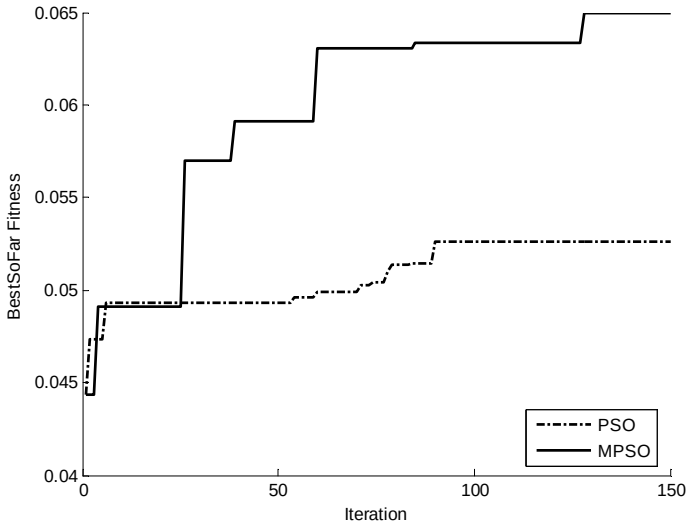

Figure 5. Convergence of MPSO compared with PSO in spectral matching of 6 storey-2 bay frame on soil type I

Table 4: Resulted scale factors for 6 storey-2 bay example on soil type I

Scaling Method	α_1	α_2	α_3	α_4	α_5	α_6	α_7	β	γ
Manual	1.000	1.000	1.000	1.000	1.000	1.000	1.000	1.411	0.070g
PSO	2.000	0.500	0.500	2.000	2.000	0.500	0.500	1.226	0.070g
MPSO	0.500	0.500	0.500	1.794	2.000	0.500	0.500	1.510	0.070g

Table 5: Spectral matching and frame sizing results for 6 storey-2 bay example on soil type I

Scaling Method	Spectral Matching Error (%)	Fitness Improvement (%)	**Sizing Method**	Minimized Weight (kg)
Manual	26.9	-	**MPSO**	2459.3
PSO	19.0	18.7	-	-
MPSO	15.4	46.6	**MPSO**	2291.2

In algorithmic point of view, the fitness improvement with respect to the initial population has been 46.6% for MPSO which is considerably greater than 18.7% for PSO. Consequently, using the optimal scale factors given by MPSO has resulted in better sizing optimization with respect to applying the manual scale factors. That is 7% improvement in the minimized columns weight from 2459.3kg to 2291.2kg.

In order to investigate the effect of target spectrum shape on the spectral matching results, the test is repeated with ICPSRDB 2800-05 design spectrum of soil type III for such a very high seismicity region. According to Fig. 6, more difference between manual scaling results and those of optimized scaling by PSO/MSPO is evident with respect to the case of stiff soil (type I) in Fig. 4. In another word, achieving spectral compatibility with such a wider target spectrum is less than the case of soil type I, resulting in more matching errors as given in Table 6. The error has growth form nearly 27% to 45% for manual scaling between the previous and current case. Similar results are observed for optimized scaling errors of

PSO and MPSO, however, less critical than the manual method. Besides, MPSO has obtained more fitness improvement than PSO considering Fig. 7 and Table 5. The wider range of error reduction has also led to more improvement in weight minimization as a result of consequent sizing; i.e. 14% improvement from 2596.4kg to 2272.8kg in this case.

Table 6: Spectral matching and frame sizing results for 6 storey-2 bay example on soil type III

Scaling Method	Spectral Matching Error (%)	Fitness Improvement (%)	**Sizing Method**	Minimized Weight (kg)
Manual/Practice	44.6	-	**MPSO**	2596.4
PSO	19.3	64.7	-	-
MPSO	17.5	81.2	**MPSO**	2272.8

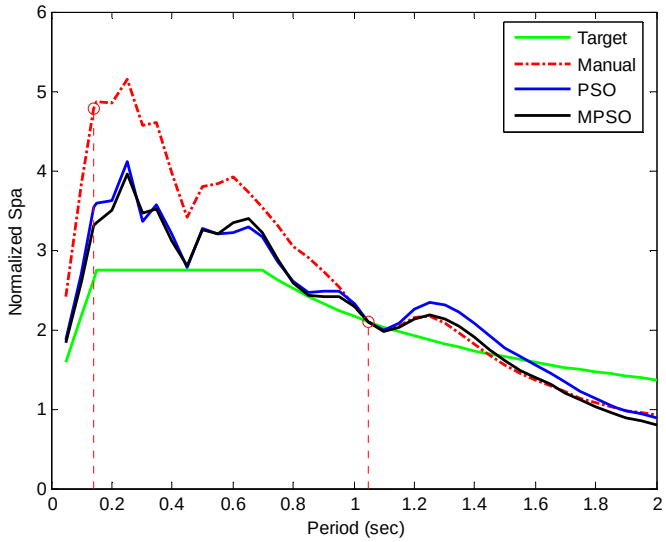

Figure 6. Comparison of various mean-scaled spectra matched for the period interval of 6 storey-2 bay frame example with the target design spectrum (5% damped - soil type III)

5.2 The 13-storey 2-bay example

Another issue to investigate is the effect of structural height and period on spectral matching and consequent sizing results. For this purpose, a 13story frame is considered in this example with the fundamental period of $1.248\,\mathrm{s}$. The corresponding period interval for spectral matching will thus be $0.250 \sim 1.872\,\mathrm{s}$ which is much wider than $0.060 \sim 0.445\,\mathrm{s}$ in the previous frame. As a result, less spectral compatibility is achieved than previous example especially in the case of soft soil (type III). It can be concluded by comparison of Fig. 8 with Fig. 9. Numerical errors reported in Tables 7 and 8 provide further support for such a conclusion.

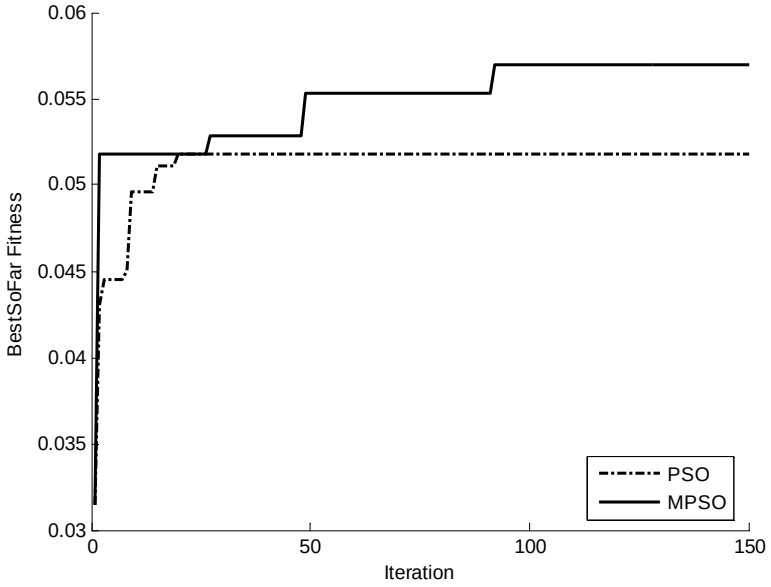

Figure 7. Convergence of MPSO compared with PSO in spectral matching of 6 storey-2 bay frame on soil type-III

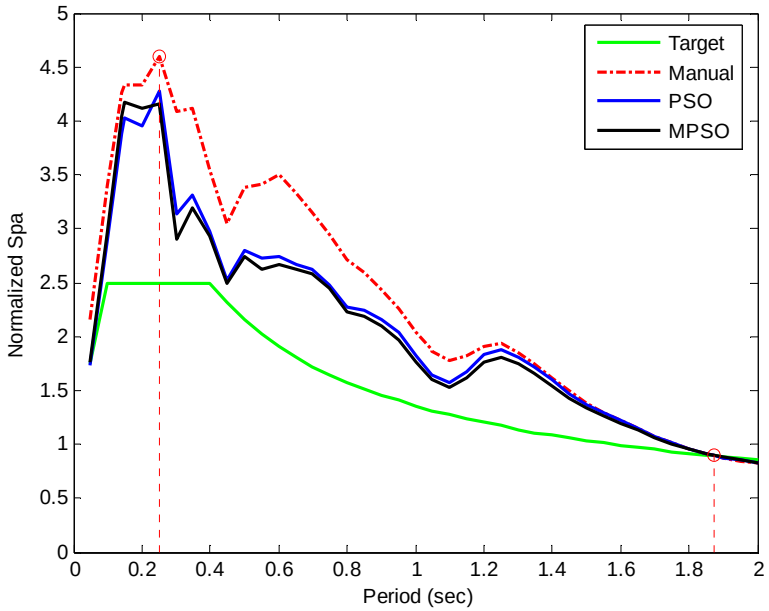

Figure 8. Comparison of various mean-scaled spectra matched for the period interval of 13 storey-2bay frame example with the target design spectrum (soil type I)

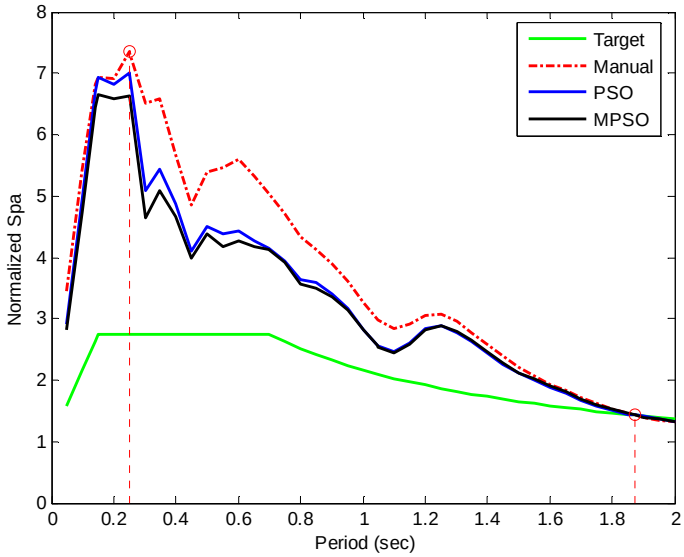

Figure 9. Comparison of various mean-scaled spectra matched for the period interval of 13storey-2bay frame example with the target design spectrum (soil type-III)

Table 7: Spectral matching and frame sizing results for 13storey-2bay example on soil type I

Scaling Method	Spectral Matching Error (%)	Fitness Improvement (%)	**Sizing Method**	Minimized Weight (kg)
Manual	48.2	-	**MPSO**	11217.8
PSO	33.9	41.4	-	-
MPSO	30.6	56.9	**MPSO**	11018.6

Table 8: Spectral matching and frame sizing results for 13storey-2bay example on soil type III

Scaling Method	Spectral Matching Error (%)	Fitness Improvement (%)	**Sizing Method**	Minimized Weight (kg)
Manual	62.3	-	**MPSO**	12095.3
PSO	44.6	27.3	-	-
MPSO	42.1	34.9	**MPSO**	11829.6

For example, relative error of manual scaling has growth from 27% to 48% for soil type I and from 45% to 62% for soil type III, respectively. However, in this example the difference between sizing results based on manual method with respect to MPSO are less than the previous lower-rise frame. Reasoning can be two fold: first; higher cardinality of search space in taller buildings requires more fitness evaluations to capture the optimal sizing design by a meta-heuristic algorithm, second; importance and contribution of the gravitational loading with respect to lateral/dynamic loads in combined member stresses and structural responses gets higher for taller buildings. The most spectral matching errors among the treated cases belonged to the 13storey example with the target design spectrum of soil type III; i.e. 62%, 45% and 42% for the manual, PSO and MPSO scaling results, respectively.

Nevertheless, superiority of MPSO over PSO in the treated examples stayed reliable as

evident from fitness improvements in Tables 5 to 8 for such a variety of frames and soil types. The reason should be searched in proper exploration and exploitation as crucial features in meta-heuristic algorithms. Population diversity trace in Fig. 10 shows that MPSO takes benefit of more DI during the search than the standard PSO in both the examples. The feature helps it in exploring more regions of the search space to access higher quality solutions in early iterations. In another view, the 4th term in Eq.8 is an additional direction pseudo-randomly scaled to construct vector-sum movements during iterations of the particle swarm optimization.

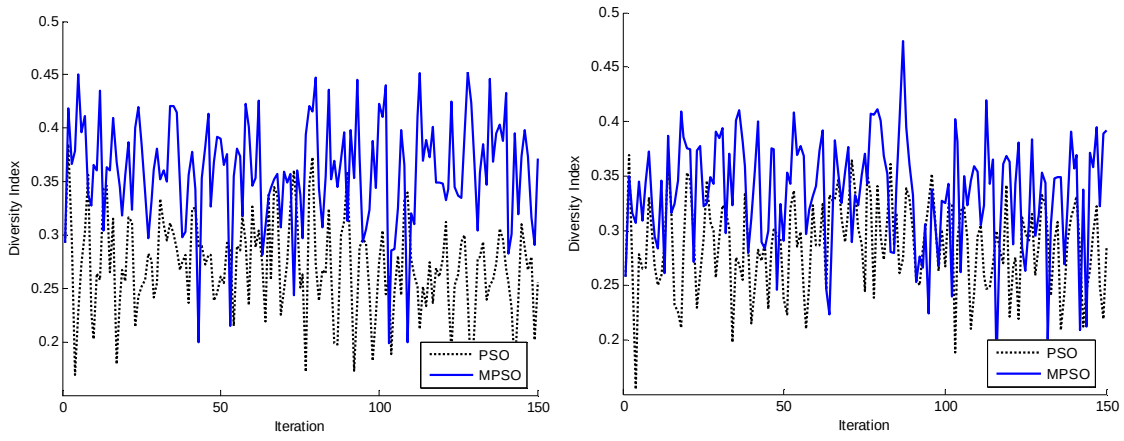

Figure 10. Diversity trace of MPSO vs. PSO in spectral matching of (a) 6 storey-2 bay and (b) 13 storey-2bay frame example

6. CONCLUSION

The present work formulated a twofold optimization for ground motion scaling and consequent sizing design of shear building frames. Since the scale factors form continuous design variables for spectral matching, the particle swarm optimization is efficiently modified and suited for this problem.

Treating examples of low-rise and medium-rise building frames, considerable ratio of such spectral-compatibility-error decrease between the optimal and equal scale factors was declared. The results confirmed necessity and benefit of spectral matching optimization.

It was also found that the compatibility error is dependent to the selected target spectrum and the employed period interval. The optimal and manual scaling errors were greater for the taller frame; as it has greater natural period leading to wider period interval for spectral matching with respect to the low-rise building example. However, the optimal results were less sensitive than those revealed by the manual practice which applies equal scale factors to different earthquake records.

The effect of target spectrum shape on spectral compatibility error was another issue investigated in this study. The error values generally were lower for stiffer soil with narrower band of frequency in its flattened peak region due to the seismic design code. The

matter was observed for both the frame examples; however, the effect of structural height and period interval is more crucial.

A number of modifications to the standard PSO have successfully improved its efficiency and effectiveness during the search. As in the treated examples, the proposed MPSO stood superior in global optimization with respect to the standard PSO. Tracing DI showed MSPO capability in maintaining higher diversity of the search agents during its progress and provided further reasoning for such a performance enhancement. In this regard, rapid capture of the near optimal solution by MSPO is found of practical interest.

Furthermore, comparisons were made to study economical impact of the proposed optimal ground motion scaling on structural weight minimization. The examples were modeled as shear buildings and analyzed under combined gravitational loading and seismic base excitation with the scaled set of accelerograms. Rigorous sizing optimization by such step-by-step numerical time-history analyses revealed that using optimal scale factors could marginally reduce the structural weight as a cost measure. However, percentage of such a structural weight minimization is not directly proportional to that of the optimal spectral matching errors.

In view of the current research, optimizing the scale factors by the proposed swarm intelligent algorithm is recommended to insure optimal scaling and proper spectral matching with the target design spectrum and take economic merit in consequent sizing design of building frames.

Acknowledgements: The first author is grateful to the Kharazmi University for the support.

REFERENCES

1. *Iranian Code of Practice for Seismic Resistant Design of Buildings*, Standard No. 2800, 3rd Ed, Building and Housing Research Center, 2005.
2. Uniform building code. *International Conference of Building Officials*, Whittier, California, 1997.
3. Bahar O, Taherpour A. Nonlinear Dynamic Behavior of RC Buildings against Accelerograms with Partial Compatible Spectrum, *14th World Conference on Earthquake Engineering* 2008, Beijing, China.
4. Clough RW, Penzien J. *Dynamics of Structures*, Third edition, Computers & Structures, Inc. Berkeley, CA, 2003.
5. Karabalis DL, Cokkinides GJ, Rizos DC, Mulliken JS. Simulation of earthquake ground motions by a deterministic approach, *Adv Eng Softw* 2000; **31**: 329–38.
6. Mukherjee S, Gupta VK. Wavelet-based generation of spectrum-compatible time-histories, *Soil Dynam Earthq Eng* 2002; **22:** 799–804.
7. Bahar O, Taherpour A. Selection of artificial spectrum compatible accelerograms for nonlinear dynamic analysis of rc buildings, *14th World Conference on Earthquake Engineering*, Beijing, China. 2008.
8. Naeim F, Lew M. On the use of design spectrum compatible time histories, *Earthq Spectra* 1995*;* **11**(1): 111-27.

9. Naeim F, Alimoradi A, Pezeshk S. Selection and scaling of ground motion time histories for structural design using genetic algorithms, *Earthq Spectra* 2004; **20**(2): 413-26.
10. Shahrouzi M, Mohamamdi A. Artificial intelligence for scaling ground motion records, *6th International Conference on Seismology and Earthquake Engineering*, Tehran, 2011.
11. Eberhart RC, Kennedy J. A new optimizer using particle swarm theory, *Proceedings of the Sixth International Symposium on Micro Machine and Human Science*, Nagoya, Japan, Piscataway, NJ: IEEE Service Center, 1995, pp. 39-43.
12. Kennedy J, Eberhart R. Swarm Intelligence, Academic Press, London, 2001.
13. Dorigo MA, Colorni A, Maniezzo V. The Ant System: optimization by a colony of cooperating agents, *IEEE Transactions on Systems, Man, and Cybernetics* 1996; **B26**(1): 29-41.
14. Clerc M, Kennedy J. The Particle Swarm-Explosion, Stability, and Convergence in a Multidimensional Complex space, *IEEE Transaction on Evolutionary Computation* 2002; **6**: 58-73.
15. Kaveh A, Talatahari S. Novel heuristic optimization method: charged system search, *Acta Mech* 2010; **213**(3-4): 267-86.
16. He S, Wu KH, Yen JY, Sanders JR, Paton RC. A particle swarm optimizer with passive congregation, *Bio Sys* 2004; **78**: 135-47.
17. Geem ZW, Kim JH, Loganathan GV. A new heuristic optimization algorithm: harmony search, *Simulation* 2001; **76**(2):60-68.
18. Rashedi E, Nezamabadipour H, Saryazdi S. GSA: a gravitational search algorithm. *Inform Sci* 2009; **179**(13): 2232–48.
19. Yang XS. Firefly algorithm stochastic test functions and design optimization, *International J Bio-inspired Comput* 2010; **2**(2): 78-84.
20. AISC-ASD89. Allowable Stress Design and Plastic Design Specifications for Structural Steel Buildings, American Institute of Steel Construction, Chicago, Illinois, 1989.
21. Pacific Earthquake Engineering Research Center, PEER Strong Motion Database, http://peer.berkeley.edu/smcat/.